

Collective modes of ultracold fermionic alkaline-earth-metal gases with $SU(N)$ symmetry

Sayan Choudhury,^{1,*} Kazi R. Islam,^{2,†} Yanhua Hou,² Jim A. Aman^{2,2} Thomas C. Killian^{2,2} and Kaden R. A. Hazzard^{2,‡}

¹*Department of Physics and Astronomy, University of Pittsburgh, Pittsburgh, Pennsylvania 15260, USA*

²*Department of Physics and Astronomy, Rice University, Houston, Texas 77251, USA*



(Received 26 January 2020; accepted 16 April 2020; published 7 May 2020)

We calculate the collective modes of ultracold trapped alkaline-earth-metal fermionic atoms, which possess an $SU(N)$ symmetry of the nuclear spin degree of freedom and a controllable N , with N as large as 10. We calculate the breathing and quadrupole modes of two-dimensional and three-dimensional harmonically trapped gases in the normal phase. We particularly concentrate on two-dimensional gases, where the shift is more accessible experimentally, and the physics has special features. We present results as a function of temperature, interaction strength, density, and N . We include calculations across the collisionless to hydrodynamic crossover. We assume the gas is interacting weakly, such that it can be described by a Boltzmann-Vlasov equation that includes both mean-field terms and the collision integral. We solve this with an approximate scaling ansatz, taking care in two dimensions to preserve the scaling symmetry of the system. We predict the collective-mode frequency shifts and damping, showing that these are measurable in experimentally relevant regimes. We expect these results to furnish powerful tools to characterize interactions and the state of alkaline-earth-metal gases, as well as to lay the foundation for future work, for example, on strongly interacting gases and $SU(N)$ spin modes.

DOI: [10.1103/PhysRevA.101.053612](https://doi.org/10.1103/PhysRevA.101.053612)

I. INTRODUCTION

Ultracold alkaline-earth-metal-like atoms such as Yb and Sr have unique properties that open new regimes of many-body physics [1–4]. One example is that their closed-shell electronic structure provides a long-lived clock state that has enabled optical clocks with a precision approaching 10^{-19} . Another example is the fermionic isotopes' large nuclear spin I , leading to a large number $N = 2I + 1$ of degenerate internal states on each atom, where any N can be produced up to $N = 6$ (in Yb) and $N = 10$ (in Sr). Equally important to the large degeneracy is the $SU(N)$ symmetry that interactions between the atoms enjoy [5–9]. Although one might naively expect that such large spins become classical, it is known that in some circumstances the large symmetry group can enhance quantum fluctuations such that they remain relevant even as $N \rightarrow \infty$ and that such fluctuations give rise to exotic phenomena such as chiral spin liquids [10,11], molecular Luttinger liquids, symmetry-protected topological phases, quantum liquids, valence-bond solid states, and magnetically ordered states [12–29], which are beginning to be explored experimentally [30–32]. In light of this, it is especially interesting to explore how the physics depends on N .

The properties of interacting Fermi gases are broadly studied, and two-dimensional (2D) gases with short-range interactions are particularly interesting for two reasons [33]. The first is that their reduced dimensionality enhances quantum and thermal fluctuations, limiting the applicability of mean-field

theory. The second is that they possess intriguing special features: an $SO(2,1)$ scaling symmetry at the classical level that is broken by a quantum anomaly for a variety of bosonic and fermionic systems [34–43] and recently predicted long-lived memory effects in homogeneous systems [44].

Collective modes—macroscopic oscillations (possibly damped) of a trapped system in response to an external perturbation—are a powerful probe of matter. They reveal information about the equation of state and quasiparticle properties, especially the quasiparticle collisions. They have therefore been central to experiments studying ultracold matter. The collective breathing (i.e., monopole) and quadrupole density modes have been measured in 2D spin-1/2 $SU(2)$ Fermi gases [45–49] and have spurred a variety of theoretical explorations [50–54]. Working in two dimensions is also beneficial for measuring collective modes of alkaline-earth-metal-like gases in experiment. The reason is that confining the system in the third dimension increases the effective interactions strength and thus increases the collective-mode frequency shifts and damping rates. This is especially important since alkaline-earth-metal atoms have no ground-state magnetic Feshbach resonances.

Given their fundamental interest and accessibility, it is interesting to study the collective modes of 2D $SU(N)$ Fermi gases. Their behavior includes the interesting behavior of spin-1/2 $SU(2)$ Fermi gases as a limiting case but goes beyond this with an additional control parameter N . Changing N may, for example, tune the strength of quantum fluctuations. Moreover, $SU(N)$ gases will also display collective oscillations of the spin degrees of freedom. These are a richer analog of the spin modes measured for $N = 2$ Fermi gases in Refs. [55–59], which have shed light on correlated quantum transport, for example, suggesting fundamental quantum bounds on hydrodynamic transport coefficients. Although we

*sc2385@cornell.edu

†Present address: Department of Physics, University of Minnesota Twin Cities, Minnesota 55455, USA.

‡kaden@rice.edu

focus in this paper on density rather than spin modes, the paper also sets up a theoretical framework for treating the latter. Initial measurements of density collective modes have been performed for $SU(N)$ Fermi gases in one dimension [60], finding strongly correlated states through a crossover from noninteracting fermions at $N = 1$ to nearly bosonic behavior at $N = 10$.

In this paper, we calculate the collective-mode frequencies and damping rates in a weakly interacting 2D $SU(N)$ Fermi gas as a function of interaction strength, temperature, and N . We focus on the breathing and quadrupole density modes. In addition to treating the weakly interacting situation, we expect the theory developed here to lay the groundwork to explore strongly interacting 2D alkaline-earth-metal-like atom gases and associated questions of spin modes and spin transport. We also briefly consider the three-dimensional (3D) gas in Sec. III D. Excitingly, recently, Ref. [61] measured the breathing-mode and quadrupole-mode frequencies and damping in a 2D $SU(N)$ Fermi gas for $N = 1, 2, \dots, 6$ in the collisionless limit. We will discuss these experiments in comparison with our calculations (along with other experimental predictions) in Sec. III C.

While our focus is on $SU(N)$ Fermi gases, several of our results are also useful for spin-1/2 $SU(2)$ gases, which occur in experiments with ultracold alkali atoms. It is worth emphasizing two results in this regard. First, our approximations are carefully designed to ensure consistency with the subtle $SO(2,1)$ scaling symmetry enjoyed by the system at the classical level (i.e., in the absence of the quantum anomaly). This symmetry is implemented consistently even in the presence of important mean-field shifts, where common alternative techniques break the symmetry and would give physically incorrect results. Second, our approximations are flexible enough to capture the quadrupole collective-mode frequency in the collisionless limit arising from mean-field interaction effects. We will discuss how our results compare to those obtained from alternative popular approximations that fail to have these desirable properties in Sec. III A.

Section II describes the experimental system we consider, the collective modes we focus on, and the theoretical framework and approximations we use to describe the nonequilibrium dynamics (a Boltzmann equation with a scaling ansatz solution). Section III presents our results for the collective modes. It describes the dependence of collective-mode frequencies and damping on system parameters: interaction strength g , N , temperature T , the number of particles N_p , and radial and transverse trap frequencies, ω_{tr} and ω_z , respectively. In particular, Sec. III C evaluates these shifts and dampings for typical experimental parameters and compares them to very recently obtained measured $SU(N)$ collective-mode properties in the collisionless limit [61]. Section III D briefly presents results for 3D gases. Section IV concludes and provides an outlook.

II. COLLECTIVE MODES AND THEORETICAL METHODS

Two-dimensional gases can be experimentally realized in ultracold alkaline-earth-metal-like atoms by directly confining them to a single layer (for example, with evanescent

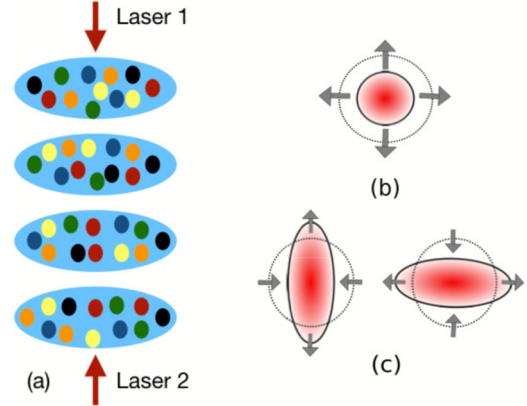


FIG. 1. Collective modes of a 2D $SU(N)$ Fermi gas. (a) Fermionic alkaline-earth-metal atoms can be confined to a single 2D layer or to an array of 2D layers formed by an optical lattice (depicted). Collective modes may be excited, for example, by suddenly changing the trap frequency. (b) and (c) The real-space deformations corresponding to the three lowest angular momentum modes, the breathing mode [in (b)], dipole mode (not depicted), and quadrupole mode [in (c)].

fields), or by creating an array of 2D systems via a one-dimensional optical lattice, as illustrated in Fig. 1(a). We will assume that the lattice is deep enough that the 2D layers are uncoupled. Also, we will assume an isotropic harmonic trap potential with trap frequency ω_{tr} .

Collective modes may be excited by suddenly changing system parameters. For collective modes of the density, like those we consider in this paper, this is often done by suddenly changing a trap frequency by a small amount ($\sim 10\%$). Which modes are excited will depend on the symmetry of this perturbation (and of the original trap). A generic perturbation excites a superposition of modes of different symmetries, but often, experiments choose perturbations to couple to modes with a single symmetry. For example, an isotropic change in trap frequencies in an isotropic trap excites only breathing modes, illustrated in Fig. 1(b). The other mode we consider in this paper is the quadrupole mode, illustrated in Fig. 1(c). To measure these modes, experiments can track *in situ* oscillations of the density profile or oscillations in time of flight, which measure the momentum distribution. Sometimes, easier-to-access observables are measured as proxies, for example, loss as a function of time, which allows one to measure the frequencies and damping rates, although it provides fewer details about the spatial and momentum-space mode structure. Recently, He *et al.* measured the breathing and quadrupole collective-mode frequencies and damping times in $SU(N)$ Yb gases confined in a one-dimensional lattice for various N up to $N = 6$ [61].

A 2D alkaline-earth-metal fermionic gas with N_p particles can be described by the grand-canonical Hamiltonian

$$H = \sum_{\alpha} \int d^2\mathbf{r} \psi_{\alpha}^{\dagger}(\mathbf{r}) \left(-\frac{\hbar^2}{2m} \nabla^2 - \mu + V(r) \right) \psi_{\alpha}(\mathbf{r}) + \frac{g_{2D}}{2} \sum_{\alpha \neq \beta} \int d^2\mathbf{r} \psi_{\alpha}^{\dagger}(\mathbf{r}) \psi_{\beta}^{\dagger}(\mathbf{r}) \psi_{\beta}(\mathbf{r}) \psi_{\alpha}(\mathbf{r}), \quad (1)$$

where $\psi_\alpha^\dagger(\mathbf{r})$ is the fermionic creation operator creating an atom at position \mathbf{r} with spin index $\alpha = 1, \dots, N$, μ is the chemical potential, m is the mass of the atom, $V(r) = m\omega_{\text{tr}}^2(x^2 + y^2)/2$ is the harmonic trap potential with frequency ω_{tr} , and g_{2D} is the interaction strength. In principle, this contact interaction must be regularized, but at the level of approximations we use throughout, this will be unnecessary. For a lattice sufficiently deep that the potential confining the atoms to the 2D plane can be described by an additive potential $m\omega_z^2 z^2/2$ (with z being the displacement perpendicular to the plane), the coupling constant is [62]

$$g_{2D} = \frac{2\pi\hbar^2}{m \ln(qa_{2D})}, \quad (2)$$

where $a_{2D} = l_z \sqrt{\pi/B} \exp(-\sqrt{\pi/2}l_z/a_{3D})$, $B = 0.915$, a_{3D} is the three-dimensional s -wave scattering length, $l_z = \sqrt{\hbar/(m\omega_z)}$, and $q \sim \sqrt{n}$ is a characteristic momentum that determines the density-dependent coupling (with n being the total density). The momentum factor q is the Fermi momentum k_F [63] and the de Broglie wavelength \sqrt{mT}/\hbar in the low- and high-temperature limits, respectively [62].

We calculate the collective modes by employing two approximations, which are reasonable in the limits considered in this paper. First, we assume that the system is weakly interacting, $1/\ln(1/na_{2D}^2) \ll 1$ (where n is the total density), its temperature is sufficiently high that there is no pairing, and the length scale over which there is any spatial coherence is small compared to the trap size (although the gas may still be deeply degenerate). In practice this means that the system must be well above the superconducting transition temperature and the length scale on which the collective modes vary must be long compared to the thermal de Broglie wavelength. This allows us to describe the system's dynamics by a Boltzmann equation, including mean-field interactions in addition to the collision integral, which governs the phase-space distribution function (defined later). The resulting Boltzmann-Vlasov (BV) equation [64] is a $(4+1)$ -dimensional partial differential-integral equation and, as such, would be extremely demanding to solve numerically.

Second, we approximate the collision integral with a relaxation-time approximation. This is an uncontrolled, but standard, approach to calculating transport and collective modes within a Boltzmann equation framework. This approximation will be explained in detail in Sec. III.

To solve the BV equation in the relaxation-time approximation, we assume an ansatz for the phase-space distribution function. The ansatz is carefully constructed to respect the $\text{SO}(2,1)$ symmetry of the system while simultaneously being flexible enough to capture the collective modes' shifts and damping. As shown in Ref. [34], this ansatz provides an exact solution to the collective modes of the BV equation in two dimensions, when the confinement is isotropic.

Under these assumptions, it is valid to apply mean-field theory to the Hamiltonian in Eq. (1) in the density channel. We assume that the density of each species is the same ($n_\alpha = n_\beta = n_0$, for all $\{\alpha, \beta\} \in \{1, \dots, N\}$), where n_0 is the density of each species. [This holds in any state that preserves the Hamiltonian's $\text{SU}(N)$ symmetry.] The mean-field Hamiltonian is

then

$$H_{\text{MF}} = \sum_\alpha \int d^2\mathbf{r} \psi_\alpha^\dagger(\mathbf{r}) \left(-\frac{\hbar^2}{2m} \nabla^2 - \mu + V(r) + U_{\text{MF}} \right) \times \psi_\alpha(\mathbf{r}), \quad (3)$$

up to irrelevant constants, and

$$U_{\text{MF}} = g_{2D} \frac{(N-1)}{N} n^{\text{tot}}(\mathbf{r}), \quad (4)$$

where $n^{\text{tot}}(\mathbf{r}) = \sum_{\alpha=1}^N n_\alpha(\mathbf{r}) = Nn_0(\mathbf{r})$ is the density of the gas at position \mathbf{r} . The chemical potential μ is chosen to give the total number of particles N_p by

$$N_p = \int d^2\mathbf{r} n^{\text{tot}}(\mathbf{r}) = N \int d^2\mathbf{r} n_0(\mathbf{r}). \quad (5)$$

To calculate the collective-mode dynamics, we will use the BV kinetic equation, which is a semiclassical method, solved by a scaling ansatz, and linearize for small displacements from equilibrium. The BV kinetic equation is accurate when the conditions outlined above for weak interactions and $k_B T \gg \hbar\omega_{\text{tr}}$ are satisfied. In this limit, we assume that the effects of quantum interference can be neglected, and quasiparticles are well defined. Furthermore, since our initial state and Hamiltonian are invariant under $\text{SU}(N)$ symmetry (i.e., we are studying the density modes), we have assumed that each spin component is described by the same semiclassical distribution function $f(\mathbf{r}, \mathbf{p}, t)$ which satisfies the BV kinetic equation,

$$\frac{\partial f}{\partial t} + \frac{\mathbf{p}}{m} \cdot \frac{\partial f}{\partial \mathbf{r}} - \frac{\partial}{\partial \mathbf{r}} [V(\mathbf{r}) + U_{\text{MF}}(\mathbf{r})] \cdot \frac{\partial f}{\partial \mathbf{p}} = -I_{\text{coll}}[f], \quad (6)$$

where $I_{\text{coll}}[f]$ is the collision integral and U_{MF} is the mean-field interaction energy. The mean-field interaction energy is given by Eq. (4), where the density $n^{\text{tot}}(\mathbf{r})$ is determined from the distribution function by

$$n^{\text{tot}}(\mathbf{r}) = N \int \frac{d^2\mathbf{k}}{(2\pi)^2} f(\mathbf{r}, \mathbf{k}), \quad (7)$$

and the collision integral $I_{\text{coll}}[f]$ is

$$I_{\text{coll}}[f_1] = \int \frac{d^2\mathbf{p}_2}{(2\pi\hbar)^2} \frac{m\hbar}{4\pi} \int_0^{2\pi} d\theta |\mathcal{T}(|\mathbf{p}_r|)|^2 (N-1) \times [f_1 f_2 (1-f_3)(1-f_4) - f_3 f_4 (1-f_1)(1-f_2)], \quad (8)$$

where we define $f_j = f(\mathbf{r}, \mathbf{p}_j)$ and \mathbf{p}_3 and \mathbf{p}_4 are given in terms of \mathbf{p}_1 , \mathbf{p}_2 , and θ as follows: θ is the angle between the outgoing relative angular momentum $\mathbf{p}_r = (\mathbf{p}_3 - \mathbf{p}_4)/2$ and the center-of-mass momentum $(\mathbf{p}_1 + \mathbf{p}_2)$, \mathbf{p}_4 is given by conservation of the center-of-mass momentum $\mathbf{p}_3 + \mathbf{p}_4 = \mathbf{p}_1 + \mathbf{p}_2$, and by the conservation of energy we obtain $|\mathbf{p}_r| = |\mathbf{p}'_r|$, where $\mathbf{p}'_r = (\mathbf{p}_1 - \mathbf{p}_2)/2$. The low-energy T matrix describing the collision between two atoms with different spins in two dimensions (in the vacuum) is given by [65]

$$\mathcal{T}(q) = \frac{4\pi}{m} \frac{1}{\ln(1/q^2 a_{2D}^2) + i\pi}. \quad (9)$$

It is hard to solve the BV equation exactly, even numerically, since this is a five-dimensional partial integro-differential equation. In this paper, we employ a scaling ansatz

for $f(\mathbf{r}, \mathbf{p}, t)$ [66–69]. Our ansatz f_{sc} is defined as

$$f_{sc}(\mathbf{r}, \mathbf{v}, t) = \Gamma(t) f^0(\mathbf{R}(t), \mathbf{V}(t)), \quad (10)$$

where $R_i(t) = \frac{r_i}{b_i(t)}$, $V_i = \frac{1}{\sqrt{b_i(t)}}(v_i - \frac{\dot{b}_i(t)}{b_i(t)}r_i)$, and $\Gamma(t) = \frac{1}{\prod_{i=1}^2 b_i(t) \sqrt{\theta_i(t)}}$, where b_i and θ_i are functions of time that will be determined to give the best solution to the BV equation. The equilibrium distribution function f^0 is defined by $I_{\text{coll}}[f^0] = 0$, which gives

$$m\mathbf{v} \cdot \frac{\partial f^0}{\partial \mathbf{r}} = \frac{\partial}{\partial \mathbf{r}}[V(r) + U_{\text{MF}}] \cdot \frac{\partial f^0}{\partial \mathbf{v}}. \quad (11)$$

As mentioned, the scaling ansatz respects the classical $\text{SO}(2, 1)$ scaling symmetry. Quantum effects can lead to a breaking of this symmetry and an anomalous correction to the breathing-mode frequency. A calculation of this quantum anomaly is beyond the scope of the BV equation, and we restrict our calculations to the regime where the BV equation is valid.

Additionally, we treat the collision integral in the relaxation-time approximation,

$$I_{\text{coll}}[f] = \frac{f - f^0}{\tau}, \quad (12)$$

where τ is the relaxation time of the collision, which is calculated in Sec. III B.

III. RESULTS

In this section, we will compute the collective-mode frequencies (Sec. III A) and damping rates (Sec. III B) of the $\text{SU}(N)$ Fermi gas. We find that the breathing-mode frequency has no dependence on the interaction strength, reflecting the $\text{SO}(2,1)$ symmetry of the system at the classical level. However, the quadrupole-mode frequencies exhibit an interaction-dependent shift and damping. We discuss how this shift and damping rates depend on N and estimate the values of these quantities for reasonable experimental parameters.

A. Collective-mode frequencies

Following Ref. [67], we compute the average moments of $R_i V_i$ and V_i^2 and obtain the following equations for b_i and θ_i :

$$\ddot{b}_i + \omega_{\text{tr}}^2 b_i - \omega_{\text{tr}}^2 \frac{\theta_i}{b_i} + \omega_{\text{tr}}^2 \xi \left(\frac{\theta_i}{b_i} - \frac{1}{b_i \prod_j b_j} \right) = 0, \quad (13)$$

$$\dot{\theta}_i + 2 \frac{\dot{b}_i}{b_i} \theta_i = -\frac{\theta_i - \bar{\theta}}{\tau}, \quad (14)$$

where $i \in \{x, y\}$, $\bar{\theta} = \frac{1}{2} \sum_i \theta_i$, and

$$\xi = \frac{\langle U_{\text{MF}} \rangle}{\langle m \omega_{\text{tr}}^2 (x^2 + y^2) \rangle}, \quad (15)$$

where $\langle \dots \rangle = \int d^2 \mathbf{r} \int \frac{d^2 \mathbf{k}}{(2\pi)^2} f^0(\dots)$. For the remainder of this section, we give our results in terms of ξ and τ . We will then calculate ξ and τ in terms of system parameters in Sec. III B.

We linearize Eqs. (13) and (14) around the equilibrium values ($b_i = 1 + \delta b_i$, $\theta_i = 1 + \delta \theta_i$) to get the collective-mode

frequencies of the density oscillations. We obtain

$$\ddot{\delta b}_j + \omega_{\text{tr}}^2 (2 + \xi) \delta b_j + \xi \omega_{\text{tr}}^2 \delta b_{\bar{j}} + \omega_{\text{tr}}^2 (\xi - 1) \delta \theta_j = 0, \quad (16)$$

$$\dot{\delta \theta}_j + 2 \delta \dot{b}_j + \frac{1}{2\tau} (\delta \theta_j - \delta \theta_{\bar{j}}) = 0, \quad (17)$$

with $\bar{j} = x$ if $j = y$ and $\bar{j} = y$ if $j = x$. The collective modes have solutions of the form $\delta b_i(t) = b_i^0 e^{i\omega t}$ and $\delta \theta_i(t) = \theta_i^0 e^{i\omega t}$. Substituting into the above equations, we obtain a set of four linear equations for b_i^0 and θ_i^0 which have nonzero solutions when the determinant of the associated matrix is zero. This gives a polynomial equation in ω that can be written as

$$\omega^2 (\omega^2 - \omega_{\text{Br}}^2) \left[(\omega^2 - \omega_{\text{cl}}^2) - \frac{i}{\omega \tau} (\omega^2 - \omega_{\text{hd}}^2) \right] = 0, \quad (18)$$

with $\omega_{\text{Br}} = 2\omega_{\text{tr}}$, $\omega_{\text{hd}} = \sqrt{2}\omega_{\text{tr}}$, and $\omega_{\text{cl}} = \sqrt{2(2 - \xi)}\omega_{\text{tr}}$.

The solution $\omega = \omega_{\text{Br}}$ to Eq. (18) corresponds to the breathing mode. It is purely real, and it is independent of ξ and τ and hence independent of all system parameters other than ω_{tr} . As mentioned, this is a consequence of the scaling symmetry of the system. In the future it will be interesting to investigate the effects of the breakdown of this symmetry due to quantum effects.

The solutions to the term in brackets in Eq. (18), $(\omega^2 - 2(2 - \xi)\omega_{\text{tr}}^2) - \frac{i}{\omega \tau} (\omega^2 - 2\omega_{\text{tr}}^2) = 0$, give the quadrupole modes' (complex) resonance frequencies. In the hydrodynamic limit, $\omega_{\text{tr}}\tau \rightarrow 0$, the solution is $\omega = \omega_{\text{hd}} = \sqrt{2}\omega_{\text{tr}}$, and in the collisionless limit, $\omega_{\text{tr}}\tau \rightarrow \infty$, the solution is $\omega = \omega_{\text{cl}} = \sqrt{2(2 - \xi)}\omega_{\text{tr}}$. The real part of the frequency smoothly crosses over between these two limits [see Fig. 2(a)], while the imaginary part is zero in these two limits, peaking in between [see Fig. 2(b)].

This behavior of the imaginary part of ω is very general and can be understood using the following argument. In the hydrodynamic limit $\omega \tau \ll 1$, there is no dissipation since frequent collisions force the deviations from local thermodynamic equilibrium, which are necessary for dissipation, to be negligible [70]. In this limit, the collective-mode frequency is

$$\omega = \omega_{\text{hd}} - i \frac{\tau (\omega_{\text{cl}}^2 - \omega_{\text{hd}}^2)}{2}. \quad (19)$$

On the other hand, in the collisionless limit $\omega \tau \gg 1$, there are few collisions per oscillation period, so dissipation is again negligible. In this limit, the collective-mode frequency is

$$\omega = \omega_{\text{cl}} - i \frac{\omega_{\text{cl}}^2 - \omega_{\text{hd}}^2}{2\tau \omega_{\text{cl}}^2}. \quad (20)$$

It is clear that the damping rate must peak somewhere between the collisionless and hydrodynamic limits. Numerically, we find that the peak occurs when $\omega \tau \sim 1$.

As detailed in the Appendix, ξ is given by

$$\xi = \frac{g_{2D}(N-1)}{2\frac{\pi\hbar^2}{m}} F\left(\frac{T}{\hbar\omega_{\text{tr}}}, \frac{N_p}{N}\right), \quad (21)$$

where $F(\frac{T}{\hbar\omega_{\text{tr}}}, \frac{N_p}{N})$ is defined as the ratio of one-dimensional integrals in Eq. (A20) and in general can be evaluated numerically. In this calculation, we have ignored the mean-field contribution to the equilibrium distribution function f^0 . This approximation gives the value of ξ to the leading order in g_{2D} .

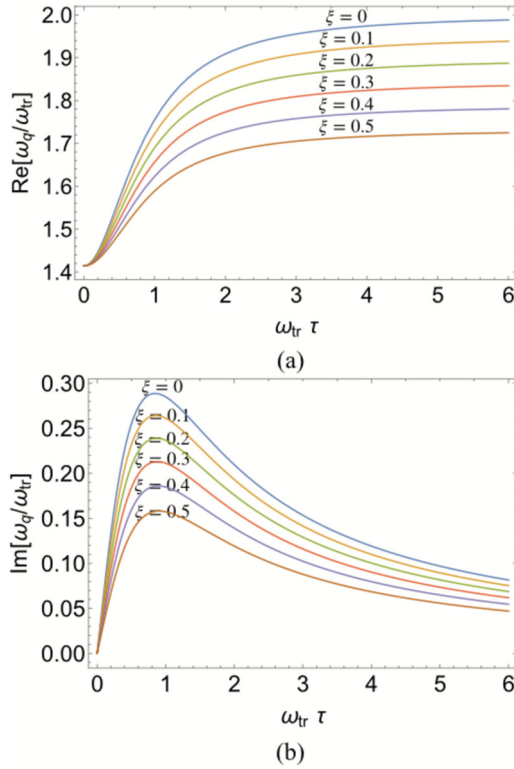


FIG. 2. Scaled quadrupole-mode frequency $\frac{\omega_q}{\omega_{tr}}$ vs scaled scattering time $\omega_{tr}\tau$. (a) Real part of the mode frequency vs scattering time and (b) imaginary part of the mode frequency vs scattering time.

It is possible to evaluate ξ analytically in the low-temperature and high-temperature limits. In the low-temperature limit, when $T \ll T_F$, ξ is

$$\xi = \frac{g_{2D}m}{2\pi\hbar^2}(N-1). \quad (22)$$

In the high-temperature limit, when $T \gg T_F$, ξ is

$$\xi = \frac{1}{8\pi} \frac{g_{2D}(N-1)}{\frac{\hbar^2}{m}} \frac{N_p}{N} \left(\frac{\hbar\omega_{tr}}{T} \right)^2. \quad (23)$$

It is interesting to note that commonly employed alternative approaches to computing the collective-mode frequencies for a 2D SU(2) Fermi gas have neglected the mean-field contribution [51,52]. Due to this approximation, neither the breathing mode nor the quadrupole modes show any mean-field shift in these calculations. Moreover, including the mean-field contribution in the Boltzmann equation in these approaches leads to an unphysical shift in the breathing-mode frequency due to the improper treatment of the SO(2,1) symmetry. As shown in the recent experiment by He *et al.* [61], accounting for the mean-field shifts in the quadrupole mode can be important, especially as N increases. Our approach captures the mean-field effects while not inducing an unphysical shift in the breathing-mode frequency.

B. Damping-rate calculation

In this section, we outline our calculations for the relaxation time τ , which employs a few common

approximations. Following Ref. [51], we write $f(\mathbf{r}, \mathbf{p}) = f_0(\mathbf{r}, \mathbf{p}) + \{f_0(\mathbf{r}, \mathbf{p})[1 - f_0(\mathbf{r}, \mathbf{p})]\} \phi(\mathbf{r}, \mathbf{p})$. Rearranging and taking moments of Eq. (12), the relaxation time is given by

$$\frac{1}{\tau} = \frac{\langle \phi^* I_{\text{coll}}[\phi] \rangle}{\langle |\phi|^2 f^0(1 - f^0) \rangle}. \quad (24)$$

To evaluate the relaxation rate, we use the following ansatz for $\phi(\mathbf{r}, \mathbf{p})$:

$$\phi = p_x^2 - p_y^2. \quad (25)$$

The linearized collision integral then reads

$$I_{\text{coll}}[f_1] = \int \frac{d^2 p_2}{(2\pi\hbar)^2} \frac{m\hbar}{4\pi} \int_0^{2\pi} d\theta |\mathcal{T}|^2 (\phi_1 + \phi_2 - \phi_3 - \phi_4) \times f_1 f_2 (1 - f_3) (1 - f_4) (N - 1). \quad (26)$$

The calculations are easiest in the high-temperature limit, when the Pauli blocking factors can be ignored. For weakly interacting Fermi gases, this approach overestimates the damping rate (by about 50%) for typical experimental temperatures ($T \sim 0.5T_F$) [51]. We note that even in an anisotropic trap, this approximation gives a lower bound on the relaxation time in the weakly interacting limit.

A more accurate estimate of the damping rate can be obtained by accounting for the Pauli blocking. This approach involves solving a six-dimensional integral numerically and overestimates the damping rate by about 10% for $N = 2$. It is possible to further systematically improve the damping-rate estimate by using an ansatz for the function ϕ that is more flexible than Eq. (25). Using a sufficiently complete basis, the result will converge to the true damping rate (within the relaxation-time approximation). The damping rate obtained using this technique is always bounded from below by the actual damping rate [47,70], so convergence may be monitored as the damping tends to its minimum, in a manner analogous to other variational calculations, e.g., the convergence of the energy to its minimum when calculating the quantum-mechanical ground-state energy.

The relaxation time in this high-temperature limit is found to be

$$\frac{1}{\tau} = \frac{N-1}{\tau_0}, \quad (27)$$

where

$$\frac{1}{\tau_0} = \frac{\pi N_p (\hbar\omega_{tr})^2}{2N\hbar k_B T} G\left(\frac{\hbar^2}{m a_{2D}^2 k_B T}\right) \quad (28)$$

and

$$G(x) = \int_0^\infty dz \frac{z^2 \exp(-z)}{\ln(x/z)^2 + \pi^2}. \quad (29)$$

C. Experimental implications

In this section, we compute the values of the mean-field shifts of the quadrupole modes and the damping rates for realistic experimental parameters. Following He *et al.* [61], we use the parameters $T = 60$ nK, $T/T_F = 0.42$, $\omega_z = 2\pi \times 59$ kHz, $\omega_{tr} = 2\pi \times 185$ Hz, $N_p/N = 100$, $T/\hbar\omega_{tr} = 5.94$, $\ln(k_F a_{2D}) = -4.3$ to estimate the quadrupole-mode shifts

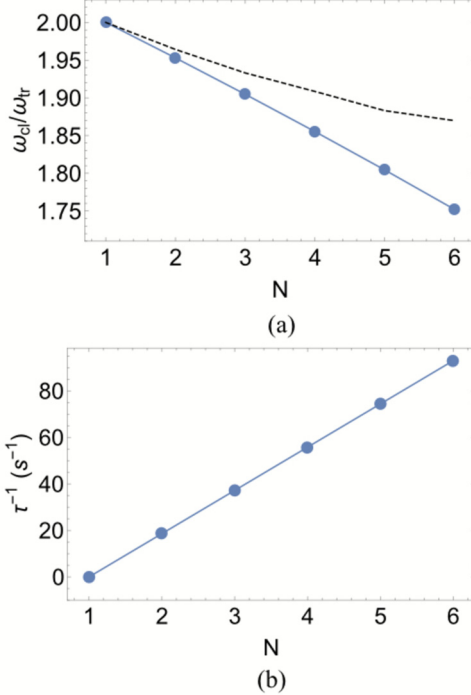


FIG. 3. (a) The ratio of the quadrupole-mode frequency to the trap frequency in the collisionless limit. The blue solid line and the black dashed line show the value of this ratio to exactly leading order in g_{2D} (neglecting the mean-field changes of the equilibrium distribution function f^0) and including the effects of mean-field interactions in f^0 , respectively. (b) The damping rate of the quadrupole modes for parameters corresponding to the experiment in Ref. [61].

and the damping rates. For these parameters, the interaction strength is

$$\frac{g_{2D}}{\frac{\hbar^2}{m}} = -\frac{2\pi}{\ln(k_F a_{2D})} = 1.461. \quad (30)$$

Using Eq. (A20), ξ , the parameter controlling the mean-field shift, is then

$$\xi = \frac{g_{2D}}{2\pi \frac{\hbar^2}{m}} (N-1) F(5.94, 100) \approx 0.093(N-1). \quad (31)$$

We compute the damping rate using Eq. (27), finding

$$\frac{1}{\tau} \approx 0.095(N-1) \frac{k_B T}{\hbar}. \quad (32)$$

Figure 3 shows the collective-mode frequency shifts and damping for the experimental parameters of Ref. [61] as a function of $N = 1, \dots, 6$. Our results for both the shifts and damping agree qualitatively with the experimental data presented in Ref. [61]. Our prediction of the frequency shift is close to the experimentally observed frequency shift when $N = 2$. We overestimate the frequency shift when $N \geq 3$, and our prediction for ω_{cl} is about 10% less than the experimentally observed value when $N = 6$. This discrepancy is likely due to our approximation of retaining fully only the leading-order contribution of g_{2D} to the frequency shift by neglecting the mean-field effects in the equilibrium distribution function. For larger N , a better estimate of ξ can

be obtained by including these mean-field effects [61]. Our damping-rate estimate shows an increase in damping rate with N , as observed experimentally. It is about 50% larger than the observed damping rate when $N = 2$. This is in agreement with previous calculations [51] and is in reasonable agreement with experiment after accounting for uncertainties in experimental parameters. However, for $N = 6$, our estimate of the damping rate is roughly a factor of 4 larger than the measurements. It will be interesting to explore in future work to what extent this discrepancy results from uncertainties in experimental parameters and to what extent it is from approximations employed in the theory.

The presence of an anisotropic trap generally leads to a coupling of the breathing and quadrupole modes [51]. This leads to a decay of the breathing mode. However, the anisotropy in recent experiments is negligible (less than 1%) [61], and therefore, we do not consider the effects of anisotropy in this paper.

D. Three-dimensional results

The previous sections computed the frequencies and damping rates of the collective modes of the 2D $SU(N)$ Fermi gas. We now briefly discuss the situation when there is no potential to confine the system to be two-dimensional (e.g., no lattice) and only a weak trapping potential in that direction. For our calculations, we assume that the gas is confined in a cylindrically symmetric harmonic potential, where $\omega_x = \omega_y = \omega_{\perp}$ and $\omega_z = \lambda \omega_{\perp}$. As outlined in Ref. [67], the quadrupole-mode frequencies are determined by the equation

$$(\omega^2 - \omega_{cl}^2) + \frac{i}{\omega_{\tau}} (\omega^2 - \omega_{hd}^2) = 0, \quad (33)$$

where $\omega_{cl}^2 = 2\omega_{\perp}^2(2 - \xi)$ and $\omega_{hd}^2 = 2\omega_{\perp}^2$, where the frequency shift ξ is given by

$$\xi = g(N-1) \frac{\langle n(r) \rangle}{\langle 2m\omega_i^2 r_i^2 \rangle} = \frac{g(N-1)}{N} \frac{3\langle n^{\text{tot}}(r) \rangle}{\langle 2m\omega_{\perp}^2 \rho^2 \rangle}, \quad (34)$$

where $\rho = \sqrt{x^2 + y^2 + \lambda^2 z^2}$. We compute the collective-mode frequencies in the low-temperature limit, where analytical results can be obtained. At zero temperature, the total density $n^{\text{tot}}(r)$ can be approximated to be

$$n^{\text{tot}}(r) = \frac{8N_p \lambda}{\pi^2 R_F^3} \left(1 - \frac{\rho^2}{R_F^2}\right)^{3/2} \Theta(R_F - r), \quad (35)$$

where $R_F = (48N_p \lambda)^{1/6} \sqrt{\hbar/(m\omega_{\perp})}$ [71]. Thus, the shift ξ is given by

$$\begin{aligned} \xi &= \frac{g(N-1)}{N} \frac{12N_p \lambda}{m\omega_{\perp}^2 \pi^2 R_F^3} \frac{\int d^3 r (1 - \frac{\rho^2}{R_F^2})^3 \Theta(R_F - r)}{\int d^3 r \rho^2 (1 - \frac{\rho^2}{R_F^2})^{3/2} \Theta(R_F - r)} \\ &= \frac{g(N-1)}{m\omega_{\perp}^2 R_F^2 N} \frac{\sqrt{3N_p \lambda (m\omega_{\perp})^3}}{\pi^2 \hbar^{3/2}} \frac{4096}{945\pi}. \end{aligned} \quad (36)$$

IV. CONCLUSIONS

We have calculated the collective modes for density oscillations of a harmonically trapped 2D $SU(N)$ Fermi gas, carefully incorporating the $SO(2,1)$ scaling symmetry. We

employed a Boltzmann-Vlasov equation, which is valid for weak interactions and when the system is large compared to spatial coherences. We treated the collisions within the relaxation-time approximation, which, while an uncontrolled approximation, is standard and captures the essential features of the hydrodynamic (and collisionless) limits. We solved this using a scaling ansatz, Eq. (10), for the semiclassical distribution function $f(\mathbf{r}, \mathbf{p})$. In contrast to other methods, for example, those based on the method of moments [72–75], the scaling ansatz preserves the $SO(2,1)$ scaling symmetry while also being flexible enough to allow for mean-field shifts.

We have shown that the magnitude of the shifts is sufficiently large to measure if the system is confined in one dimension by an optical lattice. This suggestion was borne out in recent experiments [61]. We note that in the collisionless limit, our calculations of shifts are equivalent to theirs, but ours apply across the full collisionless-hydrodynamic crossover and also capture the mode damping.

The predicted quadrupole-mode shifts agree with the experimental measurements in Ref. [61] after accounting for uncertainty in the experimental parameters. The predicted damping rate agrees with the order of magnitude observed in the experiments. For $N = 2$, the damping rates agree with about 30% relative error. However, for $N = 6$ the predicted damping rate is roughly four times the experimentally measured rate. It is possible that this arises from uncertainties in experimental parameters, which lead to a significant uncertainty already in the collective-mode shift frequencies. It is also possible that it arises from the approximations inherent in deriving and solving the BV equation. An interesting future direction will be precision experiments and calculations to pinpoint the reason for the discrepancy.

Besides calculating the weakly interacting gases' collective modes, the results in this paper lay the groundwork for several future directions with ultracold $SU(N)$ gases' collective modes and transport. One direction is to explore strongly interacting gases, for instance, to understand the shear viscosity [47] or search for novel Fermi-liquid behaviors and instabilities [76–78]. A strongly interacting regime may be achieved by tighter transverse confinement, higher densities, or optical Feshbach resonance [79–81]. In strongly interacting gases, the scaling anomaly should cause measurable effects, especially collective-mode frequency shifts, and the ability to tune N will shed new light onto its effects. In this regard, it will be interesting to employ other sensitive probes of the scale anomaly, for example, the momentum-space dynamics [82]. It will also be interesting to study physics at lower temperatures, especially when the system becomes superfluid. Although the present calculations are performed for weakly interacting normal gases, such calculations form an important point of comparison for strongly interacting and superfluid gases.

Another direction would be to explore the spin modes [83,84], which could allow a new window into strongly correlated spin transport. These modes have been explored in $N = 2$ alkali gases [55–59], but the potential spin structures are richer for larger N . A scaling ansatz similar in spirit to our approach with a spin-dependent distribution function $f_\sigma(\mathbf{r}, \mathbf{p}, t)$ has already been used to study spin-dipole modes for $SU(2)$ Fermi gases [85,86]. Furthermore, it may be

possible to generalize this scaling ansatz to include coherences. Thus, we expect that this technique can shed light on the spin collective modes of $SU(N)$ gases as well.

ACKNOWLEDGMENTS

We thank S. Natu and E. Mueller for conversations. This material is based upon work supported with funds from Welch Foundation Grant No. C-1872 and from NSF Grants No. PHY-1848304 and No. PHY-1607665. K.R.A.H. thanks the Aspen Center for Physics, which is supported by National Science Foundation Grant No. PHY-1607611, for its hospitality while part of this work was performed.

APPENDIX: CALCULATION OF ξ

Using Eqs. (4) and (15), we have

$$\xi = \frac{g_{2D}(N-1)}{m\omega_{tr}^2 N} \frac{\int d^2 \mathbf{r} n^{\text{tot}}(\mathbf{r})^2}{\int d^2 \mathbf{r} n^{\text{tot}}(\mathbf{r}) r^2}. \quad (\text{A1})$$

To calculate ξ , we need to know the form of equilibrium spatial density $n^{\text{tot}}(\mathbf{r})$ at a chemical potential set to match the total number of particles given by Eq. (5):

$$N_p = \int d^2 \mathbf{r} n^{\text{tot}}(\mathbf{r}) = N \int d^2 \mathbf{r} \int \frac{d^2 \mathbf{p}}{(2\pi)^2} f^0(\mathbf{r}, \mathbf{p}, \mu, T), \quad (\text{A2})$$

where

$$f^0 = \frac{1}{e^{(\frac{p^2}{2m} + V(\mathbf{r} + U_{MF}) - \mu)/T} + 1}. \quad (\text{A3})$$

The chemical potential μ is determined by fixing $N_p = \int d^2 \mathbf{r} n^{\text{tot}}(\mathbf{r})$. We can then numerically evaluate ξ in Eq. (A1) for the total particle number N_p at a temperature T and trap frequency ω . The mean-field contribution to f^0 can be ignored in the weakly interacting regime since it changes the density only perturbatively. In the following analysis, we set $U_{MF} = 0$. One can show that Eq. (A2) can be written as

$$\frac{N_p}{N} (\hbar\omega_{tr})^2 = \int \frac{dv du}{e^{\beta(v+u-\mu)} + 1} = -\frac{\text{Li}_2(-e^{\beta\mu})}{\beta^2}, \quad (\text{A4})$$

where $\text{Li}_\alpha(z)$ is the polylog function.

In general this equation can be solved numerically, as discussed in Sec. A3. In the next sections we analytically solve it in the high- and low-temperature limits.

1. Low-temperature limit $T \ll \hbar\omega_{tr}\sqrt{2\frac{N_p}{N}}$

For $T \rightarrow 0$, we have

$$\frac{N_p}{N} (\hbar\omega_{tr})^2 = \int_0^\infty dv \int_0^\infty du \Theta[\mu - (v + u)] \quad (\text{A5})$$

$$= \frac{\mu(T=0)^2}{2} \quad (\text{A6})$$

$$= \frac{E_F^2}{2}, \quad (\text{A7})$$

where Θ is the Heaviside theta function and E_F is the Fermi energy,

$$E_F = \hbar\omega_{\text{tr}}\sqrt{2\frac{N_p}{N}}. \quad (\text{A8})$$

The density is

$$n^{\text{tot}}(\mathbf{r}) = N \int \frac{d^2\mathbf{k}}{(2\pi)^2} f^0 = \frac{N}{2\pi} \frac{m}{\hbar^2} \int ds \frac{1}{e^{\beta(s+V(\mathbf{r})-\mu)} + 1}, \quad (\text{A9})$$

which at low temperature is

$$n^{\text{tot}}(\mathbf{r}) = \frac{N}{2\pi} \frac{m}{\hbar^2} [E_F - V(\mathbf{r})] \Theta[E_F - V(\mathbf{r})]. \quad (\text{A10})$$

Using the expression for E_F and $V(\mathbf{r})$, we get

$$n^{\text{tot}}(\mathbf{r}) = \frac{N}{4\pi} \frac{r_0^2 - r^2}{l^4} \Theta(r_0 - r), \quad (\text{A11})$$

where $r_0 = l(8\frac{N_p}{N})^{\frac{1}{4}}$ and $l = \sqrt{\frac{\hbar}{m\omega_{\text{tr}}}}$. Using Eqs. (A11) and (A1), at low temperature ($T \ll E_F$) we find

$$\xi = \frac{g_{2D}(N-1)}{\frac{2\pi\hbar^2}{m}}. \quad (\text{A12})$$

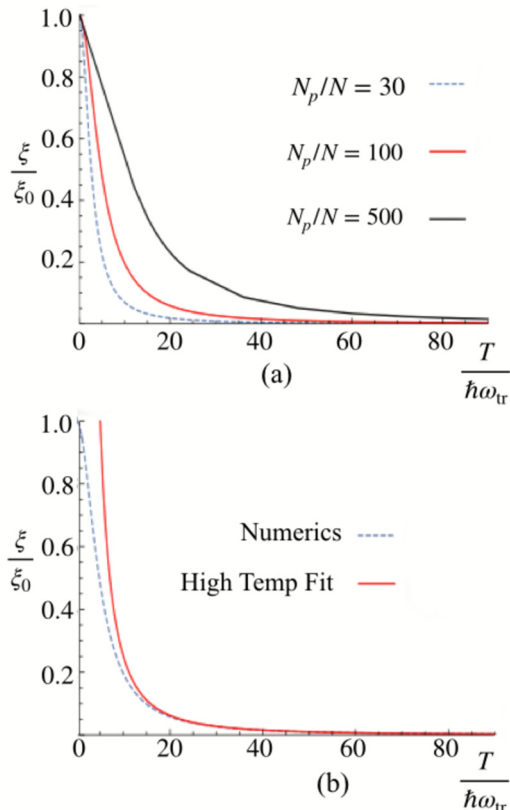


FIG. 4. (a) $\frac{\xi}{\xi_0}$ vs $\frac{T}{\hbar\omega_{\text{tr}}}$ for different values of $\frac{N_p}{N}$ and (b) numerical calculation for $\frac{\xi}{\xi_0}$ vs the theoretical calculation at the high-temperature limit for $\frac{N_p}{N} = 100$.

2. High-temperature limit $T \gg \hbar\omega_{\text{tr}} \frac{N_p}{N}$

At high temperature,

$$\frac{N_p}{N}(\hbar\omega_{\text{tr}})^2 = \int \frac{dv du}{e^{\beta(v+u-\mu)} + 1} \quad (\text{A13})$$

$$\approx \int dv du e^{\beta(\mu-v-u)} \quad (\text{A14})$$

$$= \frac{1}{\beta^2} e^{\beta\mu}, \quad (\text{A15})$$

so

$$\mu = T \ln \left[\frac{N_p}{N} \left(\frac{\hbar\omega_{\text{tr}}}{T} \right)^2 \right]. \quad (\text{A16})$$

This approximation is true only when $e^{-\beta\mu} \gg 1 \rightarrow T \gg \hbar\omega_{\text{tr}} \frac{N_p}{N}$. With this approximation, at high temperature density becomes

$$n^{\text{tot}}(\mathbf{r}) = \frac{N_p}{2\pi} \frac{\hbar\omega_{\text{tr}}}{T} \frac{e^{-\beta V(\mathbf{r})}}{l^2}, \quad (\text{A17})$$

and

$$\xi = \frac{1}{8\pi} \frac{g_{2D}(N-1)}{\frac{\hbar^2}{m}} \frac{N_p}{N} \left(\frac{\hbar\omega_{\text{tr}}}{T} \right)^2. \quad (\text{A18})$$

3. Scaling analysis

Equation (A4) implies that $\tilde{\mu} = S(\frac{N_p}{N}, \tilde{T})$, where $\tilde{\mu} \equiv \frac{\mu}{\hbar\omega_{\text{tr}}}$, $\tilde{T} \equiv \frac{T}{\hbar\omega_{\text{tr}}}$, and $S = -\tilde{T} \ln(\text{Li}_2^{-1}[-\frac{N_p}{N} \frac{1}{\tilde{T}^2}])$. The density is

$$\begin{aligned} n^{\text{tot}}(\mathbf{r}) &= \frac{N}{2\pi} \frac{m}{\hbar^2} \int ds \frac{1}{e^{\beta(s+V(\mathbf{r})-\mu)} + 1} \\ &= \frac{N}{2\pi} \frac{1}{l^2} \int d\tilde{s} \frac{1}{e^{\frac{\tilde{s}}{\tilde{T}} e^{(\frac{r}{l})^2 \frac{1}{2\tilde{T}}} e^{-\frac{\tilde{\mu}}{\tilde{T}}}} + 1} \\ &= \frac{N}{2\pi l^2} h\left(\frac{r}{l}, \tilde{T}, \frac{N_p}{N}\right), \end{aligned} \quad (\text{A19})$$

implicitly defining h on the last line. Scaling Eq. (A1), ξ is given by (Fig. 4)

$$\xi = \frac{g_{2D}(N-1)}{2\pi m\omega_{\text{tr}}^2 l^4} \frac{\int d^2\mathbf{r} h(r, \tilde{T}, \frac{N_p}{N})^2}{\int d^2\mathbf{r} r^2 h(r, \tilde{T}, \frac{N_p}{N})} \quad (\text{A20})$$

$$= \frac{g_{2D}(N-1)}{\frac{2\pi\hbar^2}{m}} F\left(\tilde{T}, \frac{N_p}{N}\right) \quad (\text{A21})$$

$$= \xi_0 F\left(\tilde{T}, \frac{N_p}{N}\right). \quad (\text{A22})$$

Here F is implicitly defined in the second line, and $\xi_0 = \frac{g_{2D}(N-1)}{\frac{\pi\hbar^2}{m}}$. One can numerically calculate $F(\tilde{T}, \frac{N_p}{N})$ in general, while the prior two sections showed that $F(0, \frac{N_p}{N}) = 1$ and $F(\tilde{T} \gg \frac{N_p}{N}, \frac{N_p}{N}) = \frac{1}{4} \frac{N_p}{N} \frac{1}{\tilde{T}^2}$.

[1] A. J. Daley, *Quantum Inf. Process.* **10**, 865 (2011).

[2] S. Stellmer, F. Schreck, and T. C. Killian, *Annual Review of Cold Atoms and Molecules* (World Scientific, Singapore, 2014), Chap. 1, pp. 1–80.

[3] M. A. Cazalilla and A. M. Rey, *Rep. Prog. Phys.* **77**, 124401 (2014).

[4] C. He, E. Hajiyyev, Z. Ren, B. Song, and G.-B. Jo, *J. Phys. B* **52**, 102001 (2019).

[5] C. Wu, J.-P. Hu, and S.-C. Zhang, *Phys. Rev. Lett.* **91**, 186402 (2003).

[6] M. A. Cazalilla, A. F. Ho, and M. Ueda, *New J. Phys.* **11**, 103033 (2009).

[7] A. V. Gorshkov, M. Hermele, V. Gurarie, C. Xu, P. S. Julienne, J. Ye, P. Zoller, E. Demler, M. D. Lukin, and A. M. Rey, *Nat. Phys.* **6**, 289 (2010).

[8] S. Stellmer, R. Grimm, and F. Schreck, *Phys. Rev. A* **84**, 043611 (2011).

[9] X. Zhang, M. Bishof, S. L. Bromley, C. V. Kraus, M. S. Safronova, P. Zoller, A. M. Rey, and J. Ye, *Science* **345**, 1467 (2014).

[10] M. Hermele, V. Gurarie, and A. M. Rey, *Phys. Rev. Lett.* **103**, 135301 (2009).

[11] M. Hermele and V. Gurarie, *Phys. Rev. B* **84**, 174441 (2011).

[12] C. Honerkamp and W. Hofstetter, *Phys. Rev. Lett.* **92**, 170403 (2004).

[13] E. V. Gorelik and N. Blümer, *Phys. Rev. A* **80**, 051602(R) (2009).

[14] T. A. Tóth, A. M. Läuchli, F. Mila, and K. Penc, *Phys. Rev. Lett.* **105**, 265301 (2010).

[15] A. Rapp and A. Rosch, *Phys. Rev. A* **83**, 053605 (2011).

[16] S. R. Manmana, K. R. A. Hazzard, G. Chen, A. E. Feiguin, and A. M. Rey, *Phys. Rev. A* **84**, 043601 (2011).

[17] P. Corboz, A. M. Läuchli, K. Penc, M. Troyer, and F. Mila, *Phys. Rev. Lett.* **107**, 215301 (2011).

[18] K. R. A. Hazzard, V. Gurarie, M. Hermele, and A. M. Rey, *Phys. Rev. A* **85**, 041604(R) (2012).

[19] L. Bonnes, K. R. A. Hazzard, S. R. Manmana, A. M. Rey, and S. Wessel, *Phys. Rev. Lett.* **109**, 205305 (2012).

[20] L. Messio and F. Mila, *Phys. Rev. Lett.* **109**, 205306 (2012).

[21] B. Bauer, P. Corboz, A. M. Läuchli, L. Messio, K. Penc, M. Troyer, and F. Mila, *Phys. Rev. B* **85**, 125116 (2012).

[22] K. Inaba and S.-I. Suga, *Mod. Phys. Lett. B* **27**, 1330008 (2013).

[23] A. Sotnikov and W. Hofstetter, *Phys. Rev. A* **89**, 063601 (2014).

[24] P. Nataf and F. Mila, *Phys. Rev. Lett.* **113**, 127204 (2014).

[25] A. Sotnikov, *Phys. Rev. A* **92**, 023633 (2015).

[26] P. Nataf, M. Lajkó, P. Corboz, A. M. Läuchli, K. Penc, and F. Mila, *Phys. Rev. B* **93**, 201113(R) (2016).

[27] G. Chen, K. R. A. Hazzard, A. M. Rey, and M. Hermele, *Phys. Rev. A* **93**, 061601(R) (2016).

[28] S. Capponi, P. Lecheminant, and K. Totsuka, *Ann. Phys. (NY)* **367**, 50 (2016).

[29] P. Nataf, M. Lajkó, A. Wietek, K. Penc, F. Mila, and A. M. Läuchli, *Phys. Rev. Lett.* **117**, 167202 (2016).

[30] C. Hofrichter, L. Rieger, F. Scazza, M. Höfer, D. R. Fernandes, I. Bloch, and S. Fölling, *Phys. Rev. X* **6**, 021030 (2016).

[31] S. Taie, R. Yamazaki, S. Sugawa, and Y. Takahashi, *Nat. Phys.* **8**, 825 (2012).

[32] H. Ozawa, S. Taie, Y. Takasu, and Y. Takahashi, *Phys. Rev. Lett.* **121**, 225303 (2018).

[33] J. Levinsen and M. M. Parish, *Annual Review of Cold Atoms and Molecules* (World Scientific, Singapore, 2015), Chap. 1, pp. 1–75.

[34] L. P. Pitaevskii and A. Rosch, *Phys. Rev. A* **55**, R853 (1997).

[35] F. Werner and Y. Castin, *Phys. Rev. A* **74**, 053604 (2006).

[36] M. Olshanii, H. Perrin, and V. Lorent, *Phys. Rev. Lett.* **105**, 095302 (2010).

[37] J. Hofmann, *Phys. Rev. Lett.* **108**, 185303 (2012).

[38] C. Gao and Z. Yu, *Phys. Rev. A* **86**, 043609 (2012).

[39] S. Moroz, *Phys. Rev. A* **86**, 011601(R) (2012).

[40] E. Taylor and M. Randeria, *Phys. Rev. Lett.* **109**, 135301 (2012).

[41] C. Chafin and T. Schäfer, *Phys. Rev. A* **88**, 043636 (2013).

[42] C. R. Ordóñez, *Phys. A (Amsterdam, Neth.)* **446**, 64 (2016).

[43] W. Daza, J. E. Drut, C. Lin, and C. Ordóñez, *Phys. Rev. A* **97**, 033630 (2018).

[44] P. J. Ledwith, H. Guo, and L. Levitov, *Ann. Phys.* **411**, 167913 (2019).

[45] E. Vogt, M. Feld, B. Fröhlich, D. Pertot, M. Koschorreck, and M. Köhl, *Phys. Rev. Lett.* **108**, 070404 (2012).

[46] T. Schäfer, *Phys. Rev. A* **85**, 033623 (2012).

[47] T. Enss, C. Küppersbusch, and L. Fritz, *Phys. Rev. A* **86**, 013617 (2012).

[48] M. Holten, L. Bayha, A. C. Klein, P. A. Murthy, P. M. Preiss, and S. Jochim, *Phys. Rev. Lett.* **121**, 120401 (2018).

[49] T. Peppler, P. Dyke, M. Zamorano, I. Herrera, S. Hoinka, and C. J. Vale, *Phys. Rev. Lett.* **121**, 120402 (2018).

[50] G. M. Bruun, *Phys. Rev. A* **85**, 013636 (2012).

[51] S. K. Baur, E. Vogt, M. Köhl, and G. M. Bruun, *Phys. Rev. A* **87**, 043612 (2013).

[52] S. Chiacchiera, D. Davesne, T. Enss, and M. Urban, *Phys. Rev. A* **88**, 053616 (2013).

[53] B. C. Mulkerin, X.-J. Liu, and H. Hu, *Phys. Rev. A* **97**, 053612 (2018).

[54] H. Hu, B. C. Mulkerin, U. Toniolo, L. He, and X.-J. Liu, *Phys. Rev. Lett.* **122**, 070401 (2019).

[55] M. Koschorreck, D. Pertot, E. Vogt, and M. Köhl, *Nat. Phys.* **9**, 405 (2013).

[56] A. B. Bardon, S. Beattie, C. Luciuk, W. Cairncross, D. Fine, N. S. Cheng, G. J. A. Edge, E. Taylor, S. Zhang, S. Trotzky, and J. H. Thywissen, *Science* **344**, 722 (2014).

[57] S. Trotzky, S. Beattie, C. Luciuk, S. Smale, A. B. Bardon, T. Enss, E. Taylor, S. Zhang, and J. H. Thywissen, *Phys. Rev. Lett.* **114**, 015301 (2015).

[58] G. Valtolina, F. Scazza, A. Amico, A. Burchianti, A. Recati, T. Enss, M. Inguscio, M. Zaccanti, and G. Roati, *Nat. Phys.* **13**, 704 (2017).

[59] T. Enss and J. H. Thywissen, *Annu. Rev. Condens. Matter Phys.* **10**, 85 (2019).

[60] G. Pagano, M. Mancini, G. Cappellini, P. Lombardi, F. Schäfer, H. Hu, X.-J. Liu, J. Catani, C. Sias, M. Inguscio, and L. Fallani, *Nat. Phys.* **10**, 198 (2014).

[61] C. He, Z. Ren, B. Song, E. Zhao, J. Lee, Y.-C. Zhang, S. Zhang, and G.-B. Jo, *Phys. Rev. Res.* **2**, 012028(R) (2020).

[62] D. S. Petrov and G. V. Shlyapnikov, *Phys. Rev. A* **64**, 012706 (2001).

[63] T. K. Ghosh and S. Sinha, *Eur. Phys. J. D* **19**, 371 (2002).

[64] We use this to refer to the Boltzmann equation with both mean-field interactions and the collision integral, but we note that some authors use this terminology to refer strictly to the collisionless equation.

[65] L. D. Landau and E. M. Lifshitz, *Quantum Mechanics: Non-relativistic Theory* (Pergamon, Oxford, 1977), Vol. 3.

[66] D. Guéry-Odelin, *Phys. Rev. A* **66**, 033613 (2002).

[67] P. Pedri, D. Guéry-Odelin, and S. Stringari, *Phys. Rev. A* **68**, 043608 (2003).

[68] H. Dong, W. Zhang, L. Zhou, and Y. Ma, *Sci. Rep.* **5**, 15848 (2015).

[69] F. Wächtler, A. R. P. Lima, and A. Pelster, *Phys. Rev. A* **96**, 043608 (2017).

[70] C. J. Pethick and H. Smith, *Bose-Einstein Condensation in Dilute Gases* (Cambridge University Press, Cambridge, 2008).

[71] D. A. Butts and D. S. Rokhsar, *Phys. Rev. A* **55**, 4346 (1997).

[72] D. Guéry-Odelin, F. Zambelli, J. Dalibard, and S. Stringari, *Phys. Rev. A* **60**, 4851 (1999).

[73] T. K. Ghosh, *Phys. Rev. A* **63**, 013603 (2000).

[74] G. M. Bruun and H. Smith, *Phys. Rev. A* **75**, 043612 (2007).

[75] S. Chiacchiera, T. Lepers, D. Davesne, and M. Urban, *Phys. Rev. A* **84**, 043634 (2011).

[76] S.-K. Yip, B.-L. Huang, and J.-S. Kao, *Phys. Rev. A* **89**, 043610 (2014).

[77] C.-H. Cheng and S.-K. Yip, *Phys. Rev. A* **95**, 033619 (2017).

[78] P. T. How and S.-K. Yip, *Phys. Rev. A* **97**, 063623 (2018).

[79] S. Blatt, T. L. Nicholson, B. J. Bloom, J. R. Williams, J. W. Thomsen, P. S. Julienne, and J. Ye, *Phys. Rev. Lett.* **107**, 073202 (2011).

[80] M. Yan, B. J. DeSalvo, B. Ramachandhran, H. Pu, and T. C. Killian, *Phys. Rev. Lett.* **110**, 123201 (2013).

[81] T. L. Nicholson, S. Blatt, B. J. Bloom, J. R. Williams, J. W. Thomsen, J. Ye, and P. S. Julienne, *Phys. Rev. A* **92**, 022709 (2015).

[82] P. A. Murthy, N. Defenu, L. Bayha, M. Holten, P. M. Preiss, T. Enss, and S. Jochim, *Science* **365**, 268 (2019).

[83] T. Enss and R. Haussmann, *Phys. Rev. Lett.* **109**, 195303 (2012).

[84] T. Enss, *Phys. Rev. A* **88**, 033630 (2013).

[85] L. Vichi and S. Stringari, *Phys. Rev. A* **60**, 4734 (1999).

[86] A. Sommer, M. Ku, G. Roati, and M. W. Zwierlein, *Nature (London)* **472**, 201 (2011).